39p

NASA TN D-1520

TECHNICAL NOTE

D-1520

AN EXPERIMENTAL INVESTIGATION OF SEVERAL ABLATION MATERIALS IN AN ELECTRIC-ARC-HEATED AIR JET

By Andrew J. Chapman

Langley Research Center
Langley Station, Hampton, Va.

NATIONAL AERONAUTICS AND SPACE ADMINISTRATION
WASHINGTON
April 1963

NATIONAL AERONAUTICS AND SPACE ADMINISTRATION

TECHNICAL NOTE D-1520

AN EXPERIMENTAL INVESTIGATION OF SEVERAL ABLATION MATERIALS IN AN ELECTRIC-ARC-HEATED AIR JET

By Andrew J. Chapman

SUMMARY

An investigation to determine the ability of several ablation materials to reduce surface heat transfer in an electric-arc-heated airstream has shown that ammonium chloride has a higher heat of ablation, and thus greater ability to reduce surface heat transfer, at stagnation enthalpy potential below 8,500 Btu/lb than Teflon, nylon, Avcoat 19, or GE-124. The trend of results indicates that, for stagnation enthalpy potential above 8,500 Btu/lb, nylon would have a higher heat of ablation than ammonium chloride because of an increased transpiration effect. Results obtained for a wide range of test stream conditions with subsonic and supersonic flow from the present investigation and several references indicate that the heat of ablation is primarily sensitive to stagnation enthalpy potential.

INTRODUCTION

Heat transfer to the surface of a vehicle during reentry to the atmosphere may be significantly reduced by injection of a gas into the boundary layer or by reradiation from a high-temperature surface. A simple method of providing gaseous injection is to cover the vehicle surface with a material which will ablate by sublimation. In addition, a high-temperature surface may be provided simultaneously with gaseous injection by using a composite material which partially vaporizes and leaves a charred surface residue.

In this investigation five ablation materials have been tested in an electric-arc-heated air-flow environment to determine their ability to reduce surface heat transfer. Four of these materials, Teflon, nylon, ammonium chloride, and Avcoat 19, are of the low-temperature subliming class. The remaining material, General Electric 124, decomposes at a low temperature and leaves a high-temperature surface residue. The ablation behavior of Teflon has been widely investigated both by experiment and analysis (for example, refs. 1 to 3). An experimental investigation of nylon is reported in reference 3, and an analytical investigation of ammonium chloride is presented in reference 4. Results of the present investigation are compared with some of the information given in these reports.

SYMBOLS

c_p	specific heat at constant pressure, Btu/lb-^{o}R
f	ratio of material vaporized to total quantity of material ablated
H_A	heat of ablation, Btu/lb
h	enthalpy, Btu/lb
h_c	heat of combustion per unit mass of oxygen, Btu/lb
L	latent heat, Btu/lb
M	molecular weight
$\dot{m}$	ablation rate, lb/ft^2-sec
N_{Le}	Lewis number
N_{Pr}	Prandtl number
p	pressure, atm
Q_A	heat required to vaporize an ablation material, Btu/lb
q_o	aerodynamic heat-transfer rate to a nonablating surface at 530^{o} R, Btu/ft^2-sec
q_o'	aerodynamic heat-transfer rate to a nonablating surface at T_A, Btu/ft^2-sec
q_c	heat transfer to a surface due to reaction of oxygen and products of ablation, Btu/ft^2-sec
q_r	radiant heat-transfer rate from a surface, Btu/ft^2-sec
q_w	aerodynamic heat-transfer rate to an ablating surface at T_A, Btu/ft^2-sec
R	radius of leading surface, ft
T	temperature, ^{o}R
t	time, sec
u	velocity component parallel to leading surface, ft/sec
v	velocity component normal to leading surface, ft/sec
v_L	regression velocity of ablating material, ft/sec

w	concentration of injected gas
x	coordinate parallel to leading surface, ft
β	boundary-layer shielding coefficient
ϵ	emissivity
μ	viscosity, lb/ft-sec
ρ	density, lb/cu ft
σ	Stefan-Boltzmann constant
τ	thickness of metal calorimeter

Subscripts:

0	initial- or room-temperature condition
1	gaseous phase of ablation material
2	air
A	ablation
c	combustion
D	dissociation
m	metal calorimeter property
s	stagnation condition or solid material
v	vaporization
w	wall condition

MATERIAL SPECIMENS

The materials tested in the course of this investigation were Teflon, nylon, ammonium chloride, Avcoat 19, and General Electric 124. Teflon and nylon were obtained commercially in solid form and ammonium chloride was obtained commercially as a powder and molded to solid form. Avcoat 19 is a proprietary product of the Avco Research and Advanced Development Division and was furnished in solid form by that company. GE-124 is also a proprietary product and was furnished in solid form by the General Electric Missile and Space Vehicle Department.

These materials were machined to cylindrical specimens with both flat and hemispherical leading surfaces as shown in figure 1. The specimens were threaded

for attachment to holders which were made of an insulating material. The holder and specimen assembly were attached to a model inserter by insulated metal extensions.

TEST FACILITY

The facility used in this investigation was the 700-kilowatt arc-powered jet at Langley Research Center. The section view in figure 2 shows the important components of the arc-heating device. Three graphite electrodes are mounted on a movable base and extend through a tank of cooling water into the arc chamber. The top of the arc chamber is formed by a graphite block containing a supersonic nozzle. The arc is struck between the electrodes and the nozzle block. Air is directed into the chamber at a controlled rate where it is heated by the arc, after which it expands through the nozzle and forms a 0.52-inch-diameter Mach number 2 stream. The contamination of the stream is approximately 7-percent carbon by weight. The electrodes are positioned automatically to maintain constant voltage at the arc.

Figure 3 shows a view of the arc jet and the inserter mechanism which positions material specimens and heating-rate probes in the stream. The inserter consists of a motor-driven wheel mounted vertically above the arc-jet nozzle exit. Specimens are mounted on the circumference of the wheel on thermally insulated extensions so that a specimen is positioned in the stream by a small rotation of the wheel. The inserter operates automatically after the jet is started so that a specimen is exposed in the stream for a preset length of time.

The range of stream conditions produced by the arc jet is given in table I. The flight region for which heating conditions are simulated is shown in figure 4.

TEST PROCEDURE

A typical test arrangement is shown in figure 5 with two heating-rate probes mounted on either side of the material specimen so that the heat-transfer rate could be measured twice before and twice after exposure of the specimen. The jet was normally operated several seconds so that stream conditions could stabilize, and then the inserter was actuated to begin positioning the heat-transfer-rate probes and specimen in the stream. The heating-rate probes were normally exposed for 0.2 second and the specimen from 3 to 5 seconds, depending on the material.

Heat-Transfer Measurement and Stream Calibration

A diagram of the probe used to measure heat-transfer rate is shown in figure 6. A size and shape identical to that of the material specimen being tested were used. The probe was made of an insulating material with a metal disk of known thermal properties, usually copper, mounted at the stagnation region. When the probe was inserted into the test stream, an approximately linear temperature rise was indicated by a thermocouple attached to the back surface of the metal disk. From this rate of temperature rise and the heat capacity of the metal disk,

the heat-transfer rate to a cold wall (assumed to be at 530° R) was determined from the following equation:

$$q_o = (c_p \rho \tau)_m \frac{dT'}{dt} \tag{1}$$

The stagnation enthalpy of the test stream was determined by using the theory of Fay and Riddell (ref. 5) for heat transfer to a blunt body of revolution. This method is described in the appendix and numerical results are shown in figure 7. The stagnation-point heat-transfer parameter $q_o\sqrt{R}$ for a hemispherical surface of radius R at nominal cold-wall conditions is given as a function of the stream stagnation enthalpy and stagnation pressure.

The stream stagnation pressure, used to obtain the stagnation enthalpy, was found by correcting the arc chamber pressure for loss across a normal shock at a Mach number of 2. The arc chamber pressure was measured continuously and recorded oscillographically.

A typical history of stream characteristics during operation of the arc jet is shown in figure 8. Values of stagnation enthalpy and temperature, obtained from figure 7 by using experimental values of heat-transfer rate and stagnation pressure, are shown. It was assumed that the enthalpy varied linearly from the initial to the final value and a point at one-half of the period of specimen exposure was taken as the average enthalpy for the specimen exposure period.

The average heat-transfer rate to the material specimen during exposure was obtained from figure 7, by using the derived average enthalpy value and the corresponding stagnation pressure. The appropriate radius, and shape correction in the case of a flat-face model, was applied to $q_o\sqrt{R}$ to obtain the cold-wall heating rate. The heating rate which would occur on the surface of a nonablating specimen at the ablation temperature of the material being tested was obtained by the following expression:

$$q_o' = q_o \frac{h_s - h_w}{h_s - h_o} \tag{2}$$

When heating-rate probes with flat leading surfaces were used, it was necessary to correct the measured heating rate to that which would occur on a hemispherical surface in order to use figure 7. The relation used was that given in reference 6 which is

$$q_o(\text{flat}) = 0.6 q_o(\text{hemisphere}) \tag{3}$$

Evaluation of Materials

The behavior of the material specimens in the test stream was recorded by a 16-millimeter camera operating at 800 to 1,200 frames per second. This

motion-picture record was the primary source for obtaining the mass loss or ablation rate of the specimen. Graphs of length change plotted against time are shown in figures 9(a) to 9(e) for each material. For all the materials the regression rate was approximately linear, and the slope of the lines represents the steady-state regression velocity v_L of the specimen surface. For a material which sublimes, the ablation rate is

$$\dot{m} = \rho v_L \tag{4}$$

Equation (4) would apply for a charring material if the thickness of the char layer were constant so that the surface of the char layer receded at the same rate as the char virgin material interface or if the char were removed mechanically soon after forming so that the surface of the virgin material was exposed, as was the case for GE-124.

The heat of ablation was obtained from the experimentally determined heat-transfer rate and ablation rate in the following manner:

$$H_A = \frac{q_o'}{\dot{m}} \tag{5}$$

The heat of ablation is a direct indication of the ability of the ablating material to reduce the heat-transfer rate which would be experienced by a non-ablating surface at the same temperature. It is shown in the appendix that the effects of reradiation and combustion may be neglected in the present tests without inducing an error greater than that due to experimental inaccuracy. The heat of ablation can be related to the material properties and stream conditions by the following approximate expression given in the appendix (eq. A11):

$$H_A = Q_A + f\beta(h_s - h_w) \tag{6}$$

The primary environmental condition in equation (6) is the enthalpy potential $h_s - h_w$ between the stagnation condition behind the normal shock and the specimen surface. The stagnation enthalpy h_s was obtained in the manner described previously in this section and the enthalpy of the test stream at the specimen surface was determined from

$$h_w = c_{p2} T_A \tag{7}$$

where the specific heat of air c_{p2} at the ablation temperature T_A of the material specimen was obtained from reference 7.

RESULTS AND DISCUSSION

The results of all tests of the materials are summarized in table II. The motion-picture records showed that Teflon, nylon, ammonium chloride, and Avcoat 19 ablated by sublimation without evidence of mechanical erosion, and that GE-124 formed a char surface layer while ablating with no evidence of a liquid or molten phase. However, it was observed that this char surface layer at the stagnation region broke off very soon after forming, as a result of either shear force, dynamic pressure, or internal pressure. A photograph of a GE-124 model before and after testing (fig. 10) shows the char residue on the side of the specimen and the removal from the nose.

All the materials attained an approximately constant regression velocity or steady-state ablation rate within 0.5 second after the beginning of exposure as shown in figure 9. This effect occurred while the stream conditions and heat-transfer rate to the model were changing. (See fig. 8.)

Heat of Ablation

The heat of ablation H_A for each material is shown as a function of stream stagnation enthalpy potential $h_s - h_w$ in figures 11 to 15. A straight line has been fitted to the set of points for each material by using the method of least squares. When the fitted line is compared with that of equation (6), the intercept corresponds to Q_A, which is the heat required to raise the material to the ablation temperature and the latent heat of decomposition. The slope of the line corresponds to β, the transpiration shielding factor.

Teflon.- The experimental values of heat of ablation for Teflon are shown as a function of $h_s - h_w$ in figure 11. A value of $Q_A = 940$ Btu/lb was obtained from reference 8. The equation which best fits the value of Q_A and the experimental data for Teflon is

$$H_A = 940 + 0.39(h_s - h_w) \tag{8}$$

Experimental and theoretical results for Teflon from references 1 and 2, and experimental results from reference 3 are also shown in figure 11 for comparison with the present test results. Agreement with the experimental results of reference 1 is close at enthalpy potential values between 2,500 and 5,000 Btu/lb. The experimental results of reference 2 show somewhat more scatter than those of the present report or of references 1 and 3. The experimental results of reference 1 have higher values of H_A above $h_s - h_w = 5{,}000$ Btu/lb than those of the present report. The derived relation (eq. (8)) for the present experimental results has a lower value of β (a somewhat lower transpiration shielding effect is thereby indicated) than the theoretical relations of references 1 and 2.

Ammonium chloride.- The experimental results for ammonium chloride are shown in figure 12. By using a value of $Q_A = 1{,}620$ Btu/lb from reference 4 with the present data, a relation corresponding to equation (6) is obtained which is

$$H_A = 1{,}620 + 0.43(h_s - h_w) \tag{9}$$

The derived relation is in close agreement with the calculated values of reference 4.

Nylon.- With the experimental results for nylon shown in figure 13, an approximate value of $Q_A = 550$ Btu/lb (estimated from an unpublished thermogravimetric analysis) has been used to derive the following relation corresponding to equation (6):

$$H_A = 550 + 0.56(h_s - h_w) \tag{10}$$

The experimental results of reference 3 essentially support the relation derived from the present data.

Avcoat 19.- A calculated value of Q_A has been used with the experimental points shown in figure 14 to obtain the following relation for Avcoat 19

$$H_A = 715 + 0.53(h_s - h_w) \tag{11}$$

The value of Q_A was obtained from information furnished by the manufacturer for a material of the same family, Avcoat 5019. This value is

$$Q_A = c_{p_s}(T_A - T_0) + L_v = 0.34 \frac{\text{Btu}}{\text{lb-}^\circ\text{R}} (1{,}160^\circ \text{ R} - 530^\circ \text{ R}) + 500 \frac{\text{Btu}}{\text{lb}}$$

$$= 715 \frac{\text{Btu}}{\text{lb}}$$

The value of $\beta = 0.53$ obtained here agreed closely with the value of 0.50 furnished by the manufacturer.

GE-124.- The results from tests of GE-124 are shown in figure 15. The expression derived from these data corresponding to equation (6) is:

$$H_A = 1{,}550 + 0.32(h_s - h_w) \tag{12}$$

Equation (12) was obtained without using a calculated value for Q_A, since sufficient information for making such a calculation was not available and the data were obtained over a range of enthalpy potential wide enough to provide a reliable trend for the relation.

As described previously, when GE-124 was exposed in the test stream, a char layer formed which broke off at the stagnation region soon after forming. In the motion-picture record it was possible to observe the surface of the uncharred

virgin material with sufficient frequency so that equation (4) could be used to determine the ablation rate.

Since only part of the ablated mass was vapor and therefore available for boundary-layer shielding, the coefficient of the boundary-layer shielding term in equation (12) is $f\beta = 0.32$ with $f < 1$. As shown in the appendix, the term $f = \dot{m}_v/\dot{m}$ represents the fraction of the total ablated mass which vaporizes, the fraction of decomposed material which remains as char layer being represented by $1 - f$.

Comparison of materials.- In the enthalpy potential range of the present tests ($h_s - h_w$ = 2,400 to 8,500 Btu/lb) the highest experimental values of heat of ablation were obtained for ammonium chloride. However, the derived relations corresponding to equation (6) for nylon and Avcoat 19 indicate that these materials will have a higher heat of ablation than ammonium chloride at enthalpy potential values greater than this range. When equation (11) for Avcoat 19 is compared with equation (9) for ammonium chloride, it is seen that the heat of ablation H_A of Avcoat 19 is predicted to be greater above $h_s - h_w$ = 9,050 Btu/lb. If equation (10) for nylon is compared with equation (9), it is shown that H_A for nylon is predicted to be greater than that of ammonium chloride above $h_s - h_w$ = 8,240 Btu/lb.

Effect of Test Stream Conditions

The Teflon data of references 1 to 3 and the present report (fig. 11) were obtained from facilities which produce widely differing test stream conditions. Some of the more important characteristics of these facilities are shown in the following table:

Data obtained in -	Source	p_s, atm	h_s, Btu/lb	Mach number	q_o, $\frac{\text{Btu}}{\text{ft}^2\text{-sec}}$ (*)	Model diameter, in.	Exposure time, sec
NASA 700-kilowatt arc jet	Present paper	3 to 10	2,700 to 8,800	2.0	1,400 to 5,000	1/4 to 1/2	3 to 6
Avco 130-kilowatt arc wind tunnel	Reference 1	.13 to .26	2,000 to 9,000	3.4	200 to 1,300	1/4 to 1/2	30
GE arc wind tunnel	Reference 2	.026	3,000 to 5,000	4.0	65 to 1,050	.667	60 to 120
NASA 1,500-kilowatt a.c. subsonic arc tunnel	Reference 3	.156 to .38	2,500 to 4,000	.16	60 to 80	3	80

*For model size indicated.

The pressure, Mach number, and the heating rates produced on the test models differ greatly; however, the range of stagnation enthalpy for the four facilities is comparable.

The agreement of the Teflon data, described previously, indicates that the heat of ablation is primarily a function of stagnation enthalpy potential as predicted by the theories of references 1, 2, 9, and 10, and is affected to a small degree if at all by stagnation pressure, Mach number, or heating rate. Although the low-pressure arc tunnels of references 1 to 3 can be more accurately controlled to produce a desired stream condition than the arc jet used for this investigation, the present results indicate that useful ablation data may be obtained from less refined facilities.

The data for each material approximately fit the linear relation of heat of ablation with stagnation enthalpy potential predicted by references 1 and 9.

SUMMARY OF RESULTS

The results of an investigation to determine the ability of several ablation materials to reduce surface heat transfer in a Mach number 2 arc-heated air stream, having a stagnation enthalpy range of 2,700 to 8,800 Btu/lb and producing heating rates of 1,400 to 5,000 Btu/ft^2-sec, may be summarized as follows:

1. The highest values of heat of ablation, and thus the greatest ability to reduce surface heat transfer, were obtained for ammonium chloride in the range of conditions covered by the present tests. However, the trend of derived relations indicated that, for stagnation enthalpy potentials greater than 8,500 Btu/lb, the heat of ablation of nylon would be greater because of an increased transpiration shielding effect.

2. The heat of ablation of the materials tested was primarily a function of stagnation enthalpy potential and may be represented approximately by a linear relation in the region of the present test conditions. Comparison of the results for Teflon with those of several other references indicated that this relation will hold for a range of test conditions varying from subsonic to supersonic and over a range of stagnation pressure from 1 to 10 atmospheres.

Langley Research Center,
National Aeronautics and Space Administration,
Langley Station, Hampton, Va., September 27, 1962.

APPENDIX

DATA ANALYSIS AND THEORY

Heat-Transfer and Test Stream Calibration

The stagnation-point heat-transfer rate to a body of revolution is given by Fay and Riddell (ref. 5) as

$$q_o = \frac{0.76}{N_{Pr}^{0.6}}(\rho_w\mu_w)^{0.1}(\rho_s\mu_s)^{0.4}\left(\frac{du}{dx}\right)_{x=0}^{0.5}(h_s - h_w)\left[1 + \left(N_{Le}^{0.52} - 1\right)\frac{h_D}{h_s}\right] \qquad (A1)$$

Brogan (ref. 11) has shown how this relation may be used to determine the stagnation enthalpy of an arc-heated wind tunnel by using measured values of q_o and values of ρ and μ, for given temperatures and pressures, obtained from a Mollier chart for equilibrium air. In reference 11 the Lewis number was assigned the value $N_{Le} = 1.4$ and Newtonian pressure distribution was assumed so that

$$\left(\frac{du}{dx}\right)_{x=0} = \frac{1}{R}\sqrt{\frac{2p_s}{\rho_s}}$$

The relation of equation (A1) was used in the present paper to determine the stagnation enthalpy except that the simplifying assumption was made that $N_{Le} = 1$. The heat-transfer rate to a hemispherical surface in the test stream, measured in the manner described in the section "Test Procedure" is then,

$$q_o = \frac{0.76}{\sqrt{R}}\,\frac{(\rho_s\mu_s)^{0.4}(\rho_w\mu_w)^{0.1}}{N_{Pr,w}^{0.6}}\left(\frac{2p_s}{\rho_s}\right)^{0.25}(h_s - h_w) \qquad (A2)$$

Values of $q_o\sqrt{R}$ were calculated from equation (A2) for constant stagnation pressure and temperature and plotted as shown in figure 7. The viscosity and Prandtl number were obtained from reference 7 and values of density and enthalpy were obtained from reference 12. The wall enthalpy h_w in equation (A2) was determined at 530° R so that the heat-transfer rate in figure 7 is to a surface at standard ambient temperature or cold-wall conditions.

The stagnation enthalpy of the test stream was determined from figure 7 by using the experimental value of q_o, the radius R of the heating-rate probes, and the stagnation pressure p_s obtained from the measured arc chamber pressure by applying a correction for the loss across a normal shock at a Mach number of 2. This method for obtaining the stream characteristics was checked by measuring the temperature of the bow shock wave in front of the specimen with the spectrographic technique described in reference 13. The theoretically derived value of stagnation temperature varied less than 7.5 percent from the measured value.

Ablation

The nomenclature used in this report is essentially in agreement with that used in references 1, 9, and 10 except that modifications have been made where necessary to suit the materials and conditions of the present investigation.

An energy balance at the surface of an ablating material may be expressed as

$$q_w - q_r + q_c = Q_A \dot{m} \tag{A3}$$

where q_w is the rate of heat transfer to the surface due to convection, q_r is the rate at which heat is radiated from the surface, and q_c is the rate of heat transfer to the surface due to the reaction of oxygen with the gaseous products of ablation.

The heat required to raise the material to the ablation temperature and the latent heat of vaporization are included in the term Q_A. Since exposure times for the present tests were very short (3 to 5 seconds), conduction within the material was neglected and the expression for Q_A was assumed to be

$$Q_A = c_{p_s}(T_A - T_0) + L_v \tag{A4}$$

It was considered that all the materials in this investigation completely decomposed at a temperature T_A and at a rate $\dot{m}$, whether the products of decomposition were completely gaseous or composed of gas and char.

As shown in references 1, 9, and 10, the rate of convective heat transfer to the surface of an ablating material is less than the convective heat-transfer rate q_o' that would be experienced by a nonablating surface at the same temperature as the ablating surface, by the amount of the heat absorbed in the boundary layer by gaseous injection:

$$q_w = q_o' - \beta(h_s - h_w)\dot{m}_v \tag{A5}$$

For a material which sublimes, the rate of gaseous injection is equal to the total rate of mass loss ($\dot{m}_v = m$), and for a charring material the rate of gaseous injection is less than the total mass loss ($\dot{m}_v < \dot{m}$), the difference being accounted for by the formation of char. The fraction of stagnation enthalpy potential absorbed in a laminar boundary layer by the gaseous products of ablation is given in reference 1 as a function of the ratio of the molecular weight of air to that of the injected gas,

$$\beta = 0.6\left(\frac{29}{M_1}\right)^{0.26} \tag{A6a}$$

and in reference 9 as a function of the ratio of the specific heat of the injected gas to that of air,

$$\beta = \left[1 + \left(\frac{c_{p_1}}{c_{p_2}} - 1\right)w\right]\left(1 - \frac{1}{3} N_{Pr}^{-0.6}\right) \tag{A6b}$$

By combining equations (A3) and (A5) the heat-transfer rate to a nonablating surface, which corresponds to the calorimeter measurements described in the text, may be expressed as

$$q_o' = \frac{Q_A\dot{m} + \beta(h_s - h_w)\dot{m}_v}{1 + \frac{q_c - q_r}{q_o'}} \tag{A7}$$

The heat of ablation which is determined from the experimentally measured quantities q_o' and $\dot{m}$ is then

$$H_A = \frac{q_o'}{\dot{m}} = \frac{Q_A + f\beta(h_s - h_w)}{1 + \frac{q_c - q_r}{q_o'}} \tag{A8}$$

The term $f = \dot{m}_v/\dot{m}$ in equation (A8) is the fraction of the total ablated mass which vaporizes and which is available for boundary-layer shielding. For the two types of materials considered in this investigation, $f = 1$ for materials which sublime and $f < 1$ for materials which partially vaporize and leave a charred surface residue. In the second case the fraction of ablated material which becomes char is represented by $1 - f$.

It may be seen from equation (A8) that the apparent value of H_A determined from experiment would be increased by the effect of reradiation q_r and decreased by the effect of combustion q_c. An upper bound estimate of these effects can be made from the following calculations of q_r/q_o' and q_c/q_c'.

The rate at which heat is radiated from a surface is given by

$$q_r = \epsilon\sigma T_A^4 \tag{A9}$$

It was assumed that the maximum emissivity for any material tested was $\epsilon = 0.8$. When it is considered that the highest surface temperature of the materials tested

was approximately $T_A = 1{,}500^\circ$ R, and that the range of heating rate for practically all tests was $q_o' = 2{,}000$ to $3{,}000$ Btu/ft^2-sec, an approximate maximum value is $q_r/q_o' < 1 \times 10^{-3}$.

In reference 1 the maximum heat transfer due to the heat of reaction h_c of oxygen and injected vapor is given as

$$q_c = q_w\left(0.21\,\frac{h_c}{h_s - h_w}\right) \tag{A10}$$

For Teflon, as an example, if a value of either $h_c = 10{,}000$ Btu/lb (ref. 1) or $h_c = 9{,}380$ Btu/lb (ref. 2) is used with values of $q_w = Q_A\dot{m} = 1{,}000$ (an approximation from the experimental data), and $h_s - h_w = 5{,}000$ Btu/lb in equation (A10), then $q_c/q_o' < 0.25$ for the range of q_o' mentioned previously. This result shows that the effect of combustion could be more significant than that of radiation, especially at low enthalpy and surface temperature. However, if there had been appreciable combustion in the present tests, there should have been a consistent decrease in the values of H_A at lower $h_s - h_w$, in figure 11 as predicted in references 1 and 2 and shown by the curve in figure 11. The Teflon data shown in figure 11 do not appear to follow this trend, the variation being entirely attributable to experimental scatter. In addition, the 7-percent carbon contamination in the stream could react with oxygen, and thus reduce that available to react with the gaseous products of ablation. However, it would be necessary to make tests at lower enthalpy to determine accurately the effect of combustion.

From the assumptions shown, it appears that the effects of radiation and combustion in the present tests are insignificant and can be neglected without inducing an error greater than that due to experimental inaccuracy. Equation (A8) then becomes

$$H_A = \frac{q_o'}{\dot{m}} = Q_A + f\beta(h_s - h_w) \tag{A11}$$

which was used for comparison with the experimental data.

REFERENCES

1. Georgiev, Steven, Hidalgo, Henry, and Adams, Mac C.: On Ablating Heat Shields for Satellite Recovery. Res. Rep. 65 (AFBMD-TR-59-7), Avco-Everett Res. Lab., July 1959.

2. Steg, Leo: Materials for Re-Entry Heat Protection of Satellites. [Preprint] 836-59, American Rocket Soc., June 1959.

3. Brown, Ronald D., and Levin, L. Ross: A 6-Inch Subsonic High-Temperature Arc Tunnel for Structures and Material Tests. NASA TN D-1621, 1963.

4. Welker, Jean E.: Comparison of Theoretical and Experimental Values for the Effective Heat of Ablation of Ammonium Chloride. NASA TN D-553, 1960.

5. Fay, J. A., and Riddell, F. R.: Theory of Stagnation Point Heat Transfer in Dissociated Air. Jour. Aero. Sci., vol. 25, no. 2, Feb. 1958, pp. 73-85, 121.

6. Stoney, William E., Jr.: Local Heat Transfer to Blunt Noses at High Supersonic Speeds. NACA RM L57D25c, 1957.

7. Hansen, C. Frederick: Approximations for the Thermodynamic and Transport Properties of High-Temperature Air. NASA TR R-50, 1959. (Supersedes NACA TN 4150.)

8. Wentink, Tunis, Jr.: High Temperature Behavior of Teflon. Res. Rep. 55 (AFBMD-TN-59-15), Avco-Everett Res. Lab., July 1959.

9. Roberts, Leonard: A Theoretical Study of Stagnation-Point Ablation. NASA TR R-9, 1959. (Supersedes NACA TN 4392.)

10. Swann, Robert T., and South, Jerry: A Theoretical Analysis of Effects of Ablation on Heat Transfer to an Arbitrary Axisymmetric Body. NASA TN D-741, 1961.

11. Brogan, Thomas R.: Electric Arc Gas Heaters for Re-Entry Simulation and Space Propulsion. [Preprint] 724-58, American Rocket Soc., Nov. 1958.

12. Moeckel, W. E., and Weston, Kenneth C.: Composition and Thermodynamic Properties of Air in Chemical Equilibrium. NACA TN 4265, 1958.

13. Greenshields, David H.: Spectrographic Temperature Measurements in a Carbon-Arc-Powered Air Jet. NASA TN D-169, 1959.

TABLE I

TYPICAL RANGE OF OPERATING CONDITIONS FOR LANGLEY 700-KILOWATT ARC-HEATED AIR JET

Pressure range	Arc chamber pressure, atm	Stagnation pressure, p_s, atm	Stagnation enthalpy, h_s, Btu/lb	Stagnation temperature, T_s, ^oR	Heat-transfer rate (1/2-in.-diam. hemisphere, cold wall), Btu/ft^2-sec	Mach number	Nozzle throat diameter, in.	Test stream diameter, in.
Low	4.2	3	3,600 to 6,300	7,900 to 11,300	1,600 to 3,100	2	0.4	0.52
Intermediate	6.9	5	2,700 to 8,800	6,500 to 12,600	1,400 to 4,400	2	.4	.52
High	13.9	10	3,000 to 5,500	7,500 to 11,000	2,600 to 5,000	2	.4	.52

TABLE II

SUMMARY OF TEST RESULTS

(a) Teflon

Test	Model diameter, in.	Model shape	Heat-transfer parameter, $q_o\sqrt{R}$, $Btu/ft^{3/2}$-sec	Stagnation pressure, p_s, atm	Stagnation temperature, T_s, ^oR	Stagnation enthalpy potential, $h_s - h_w$, Btu/lb (a)	Heat-transfer rate (hot wall), q_o', Btu/ft^2-sec (b)	Ablation rate, $\dot{m}$, lb/ft^2-sec	Heat of ablation, H_A, Btu/lb
1	1/2	Hemispherical	360	8.10	7,750	2,700	2,270	1.005	2,260
2	1/2	Hemispherical	310	5.45	7,900	2,950	1,970	.890	2,210
3	1/2	Hemispherical	380	4.95	9,350	3,950	2,470	.918	2,690
4	1/2	Flat	640	4.86	11,700	6,600	2,570	.788	3,260
5	1/4	Flat	403	11.80	7,740	2,700	2,150	1.100	1,960
6	1/4	Flat	460	5.88	9,700	4,300	2,540	1.100	2,310
7	1/4	Flat	476	6.75	9,700	4,200	2,630	1.100	2,390
8	1/4	Flat	527	6.94	10,100	4,450	2,920	1.070	2,730
9	1/4	Flat	552	7.22	10,400	4,700	3,070	1.04	2,950

[a] h_w = 400 Btu/lb.

[b] T_A = 1,500° R (average of values given in refs. 2 and 9).

TABLE II.- Continued

SUMMARY OF TEST RESULTS

(b) Ammonium chloride

Test	Model diameter, in.	Model shape	Heat-transfer parameter, $q_o\sqrt{R}$, $Btu/ft^{3/2}$-sec	Stagnation pressure, p_s, atm	Stagnation temperature, T_s, ^oR	Stagnation enthalpy potential, $h_s - h_w$, Btu/lb (a)	Heat-transfer rate (hot wall), q_o', Btu/ft^2-sec (b)	Ablation rate, $\dot{m}$, lb/ft^2-sec	Heat of ablation, H_A, Btu/lb
1	1/2	Hemispherical	370	5.15	9,000	3,850	2,460	0.79	3,110
2	1/2	Hemispherical	280	5.80	7,560	2,800	1,830	.68	2,690
3	1/2	Hemispherical	620	12.00	9,900	4,300	4,140	1.30	3,180
4	1/2	Hemispherical	350	8.40	7,380	2,700	2,280	.695	3,290
5	1/2	Hemispherical	440	4.85	10,100	4,600	2,940	.775	3,800
6	1/4	Flat	700	4.90	12,200	7,500	4,030	.76	5,300
7	1/4	Flat	1,000	7.70	13,000	8,500	5,780	.975	5,930
8	1/4	Flat	480	3.40	11,300	6,000	2,740	.646	4,250
9	1/4	Flat	520	5.25	11,000	5,400	2,970	.807	3,680
10	1/4	Flat	520	6.90	10,100	4,600	2,950	.988	2,990
11	1/4	Flat	600	10.00	9,720	4,150	3,390	1.16	2,920

[a] h_w = 300 Btu/lb.
[b] T_A = 1,100° R (ref. 4).

TABLE II.- Continued

SUMMARY OF TEST RESULTS

(c) Nylon

Test	Model diameter, in.	Model shape	Heat-transfer parameter, $q_o\sqrt{R}$, Btu/ft$^{3/2}$-sec	Stagnation pressure, p_s, atm	Stagnation temperature, T_s, ^oR	Stagnation enthalpy potential, $h_s - h_w$, Btu/lb (a)	Heat-transfer rate (hot wall), q_o', Btu/ft^2-sec (b)	Ablation rate, $\dot{m}$, lb/ft^2-sec	Heat of ablation, H_A, Btu/lb
1	1/2	Hemispherical	430	5.15	9,900	4,350	2,860	0.85	3,370
2	1/2	Hemispherical	360	5.50	8,640	3,600	2,390	1.04	2,290
3	1/2	Flat	480	5.14	9,540	4,900	1,930	.625	3,100
4	1/2	Flat	420	4.21	10,250	4,750	1,690	.510	3,310
5	1/4	Flat	530	4.62	11,200	5,600	3,030	.803	3,770
6	1/4	Flat	560	5.10	11,300	5,800	3,200	.816	3,920
7	1/4	Flat	630	7.14	11,300	5,550	3,590	.851	4,220
8	1/4	Flat	690	9.53	10,800	5,100	3,920	1.030	3,810
9	1/4	Flat	230	4.48	6,840	2,400	1,260	.698	1,810
10	1/4	Flat	220	2.54	7,920	3,300	1,240	.698	1,770
11	1/4	Flat	390	5.70	9,180	3,900	2,200	.886	2,480
12	1/4	Flat	440	6.73	9,000	3,850	2,480	.950	2,610

[a] h_w = 300 Btu/lb.

[b] T_A = 1,200° R (thermogravimetric analysis).

TABLE II.- Continued

SUMMARY OF TEST RESULTS

(d) Avcoat 19

Test	Model diameter, in.	Model shape	Heat-transfer parameter, $q_o\sqrt{R}$, $Btu/ft^{3/2}$-sec	Stagnation pressure, p_s, atm	Stagnation temperature, T_s, ^oR	Stagnation enthalpy potential, $h_s - h_w$, Btu/lb (a)	Heat-transfer rate (hot wall), q'_o, Btu/ft^2-sec (b)	Ablation rate, $\dot{m}$, lb/ft^2-sec	Heat of ablation, H_A, Btu/lb
1	1/2	Hemispherical	720	4.26	12,400	8,000	4,900	0.917	5,340
2	1/2	Hemispherical	410	3.63	10,500	5,050	2,750	.920	2,990
3	1/2	Hemispherical	355	4.25	9,000	3,900	2,360	.869	2,720
4	1/2	Hemispherical	370	4.90	9,180	4,000	2,470	.875	2,820

[a] h_w = 300 Btu/lb.

[b] T_A = 1,160° R (furnished by manufacturer).

TABLE II.- Concluded

SUMMARY OF TEST RESULTS

(e) General Electric 124

Test	Model diameter, in.	Model shape	Heat-transfer parameter, $q_o\sqrt{R}$, $Btu/ft^{3/2}$-sec	Stagnation pressure, p_s, atm	Stagnation temperature, T_s, ^oR	Stagnation enthalpy potential, $h_s - h_w$, Btu/lb (a)	Heat-transfer rate (hot wall), q_o', Btu/ft^2-sec (b)	Ablation rate, $\dot{m}$, lb/ft^2-sec	Heat of ablation, H_A, Btu/lb
1	1/2	Hemispherical	410	5.00	9,720	4,300	2,740	0.885	3,100
2	1/2	Hemispherical	240	5.40	6,840	2,350	1,560	.727	2,140
3	1/2	Hemispherical	420	4.40	9,900	4,600	2,820	.820	3,440
4	1/4	Flat	620	6.40	11,200	5,600	3,540	1.06	3,340
5	1/2	Flat	400	5.44	9,360	4,000	1,600	.610	2,620
6	1/2	Flat	800	5.50	12,600	8,100	3,260	.805	4,050

[a] h_w = 300 Btu/lb.

[b] T_A = 1,100° R (thermogravimetric analysis).

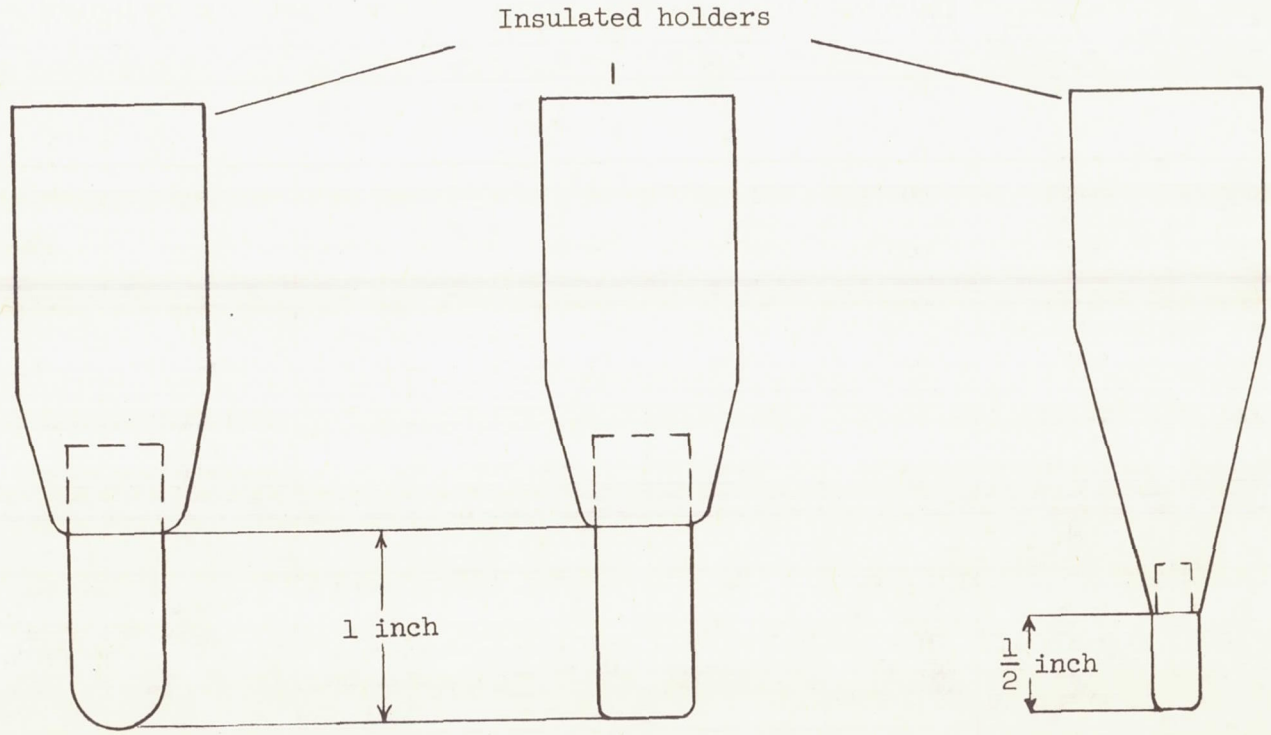

1/2-inch-diameter hemispherical leading surface

1/2-inch-diameter flat leading surface

1/4-inch-diameter flat leading surface

Figure 1.- Material specimens.

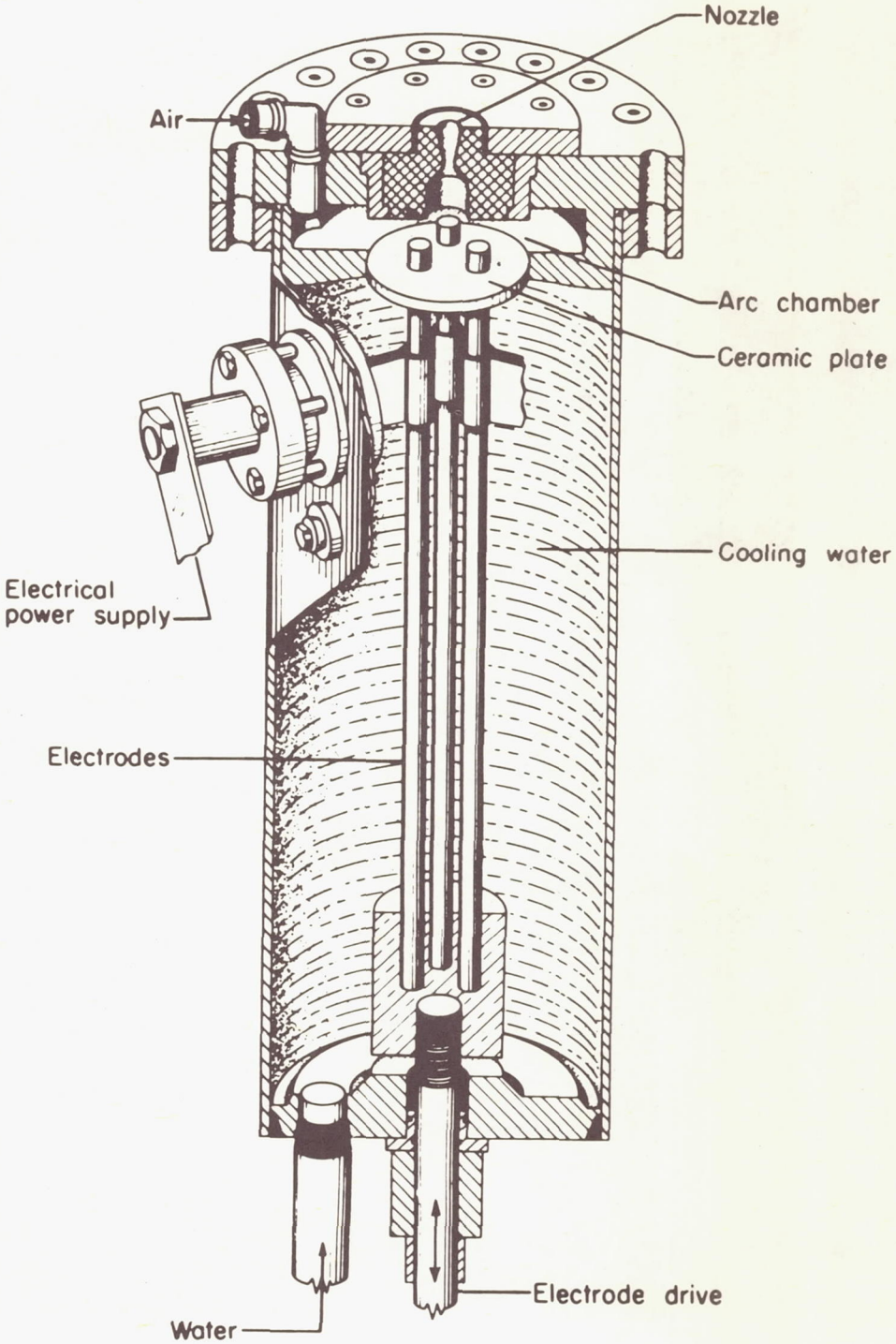

Figure 2.- 700-kilowatt electric-arc-powered air jet.

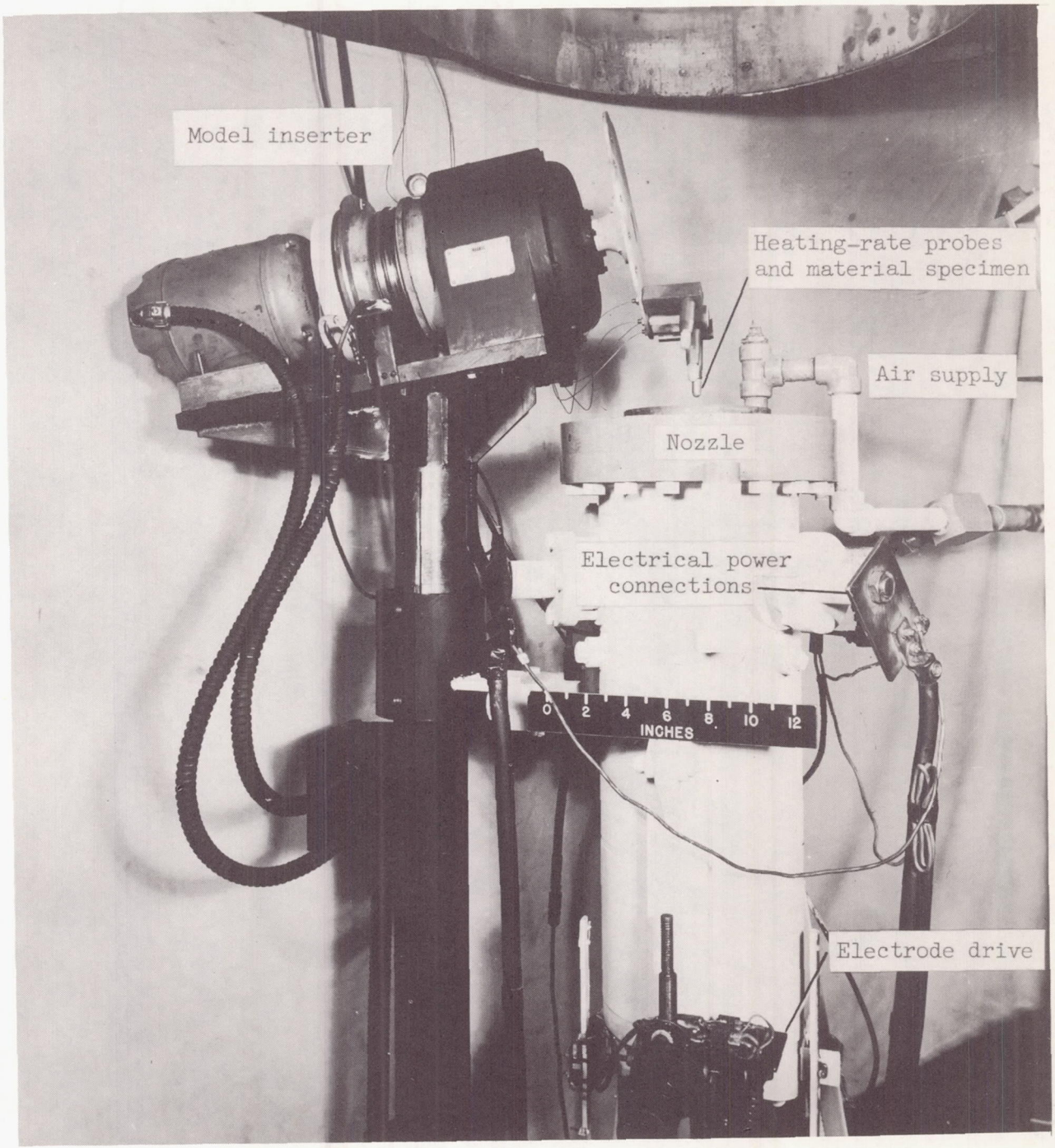

Figure 3.- Electric-arc-powered air jet and specimen inserter. L-60-1754.1

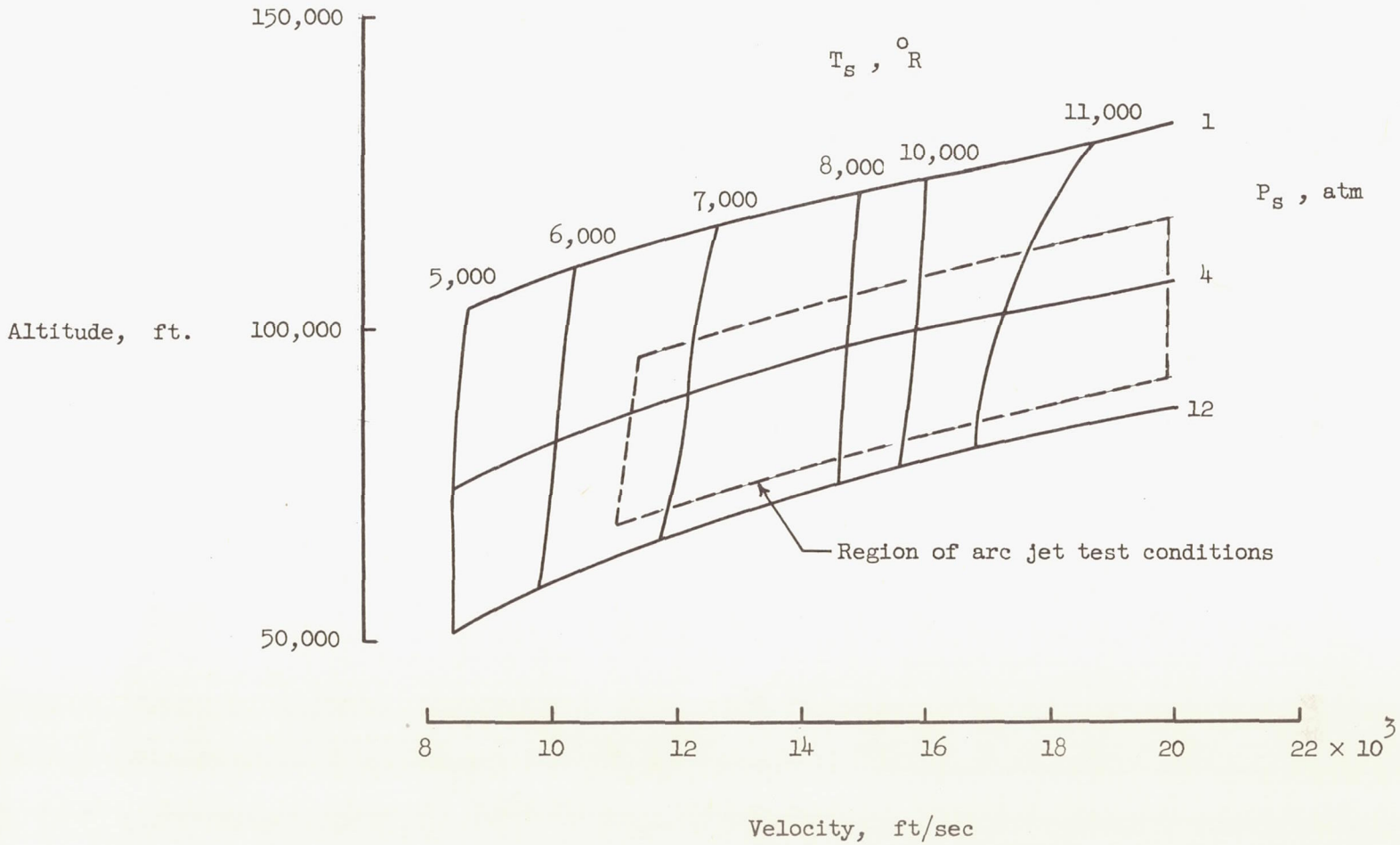

Figure 4.- Flight region for which heating conditions are simulated by arc jet.

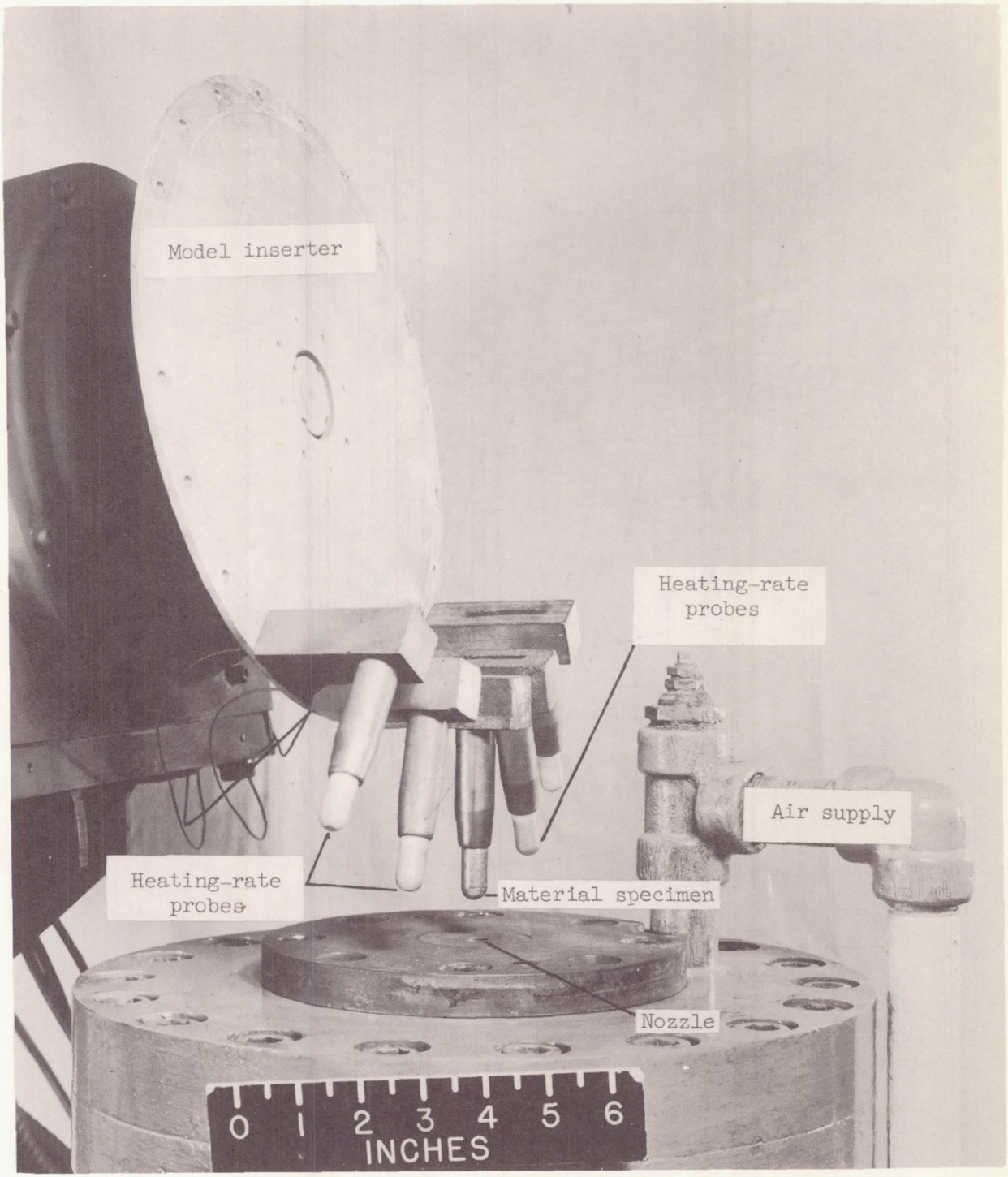

L-60-1758.1

Figure 5.- Experimental arrangement of material specimen and heating-rate probes.

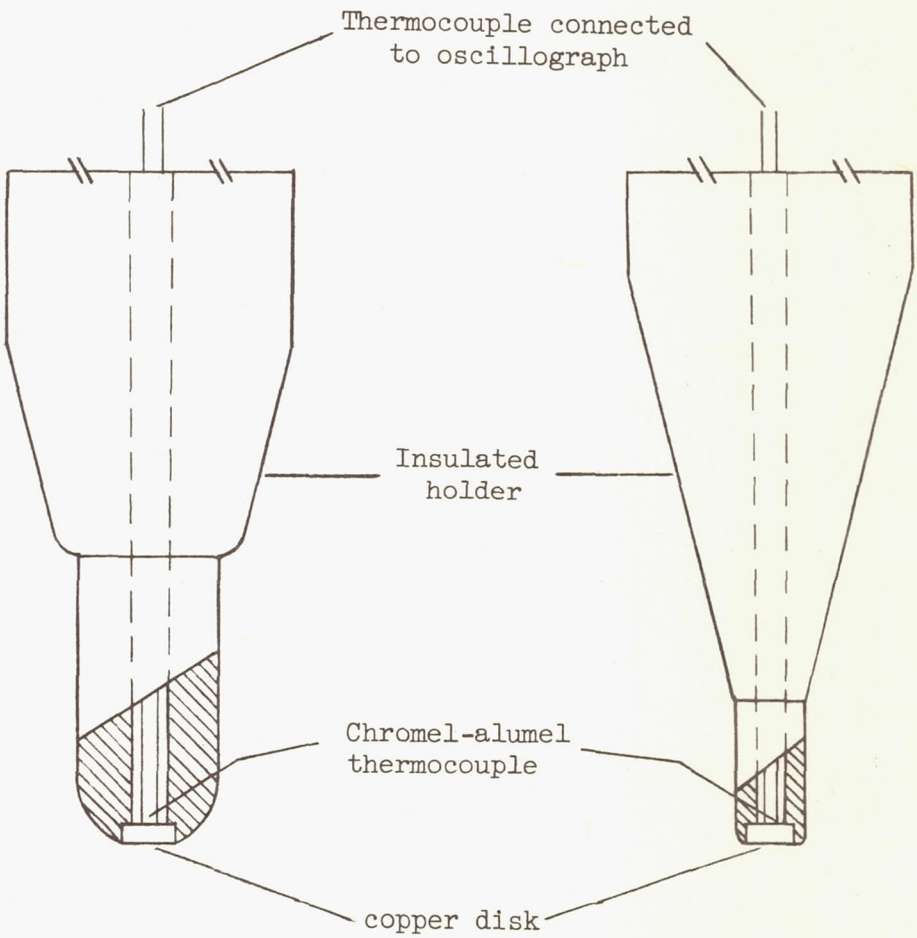

Figure 6.- Heating-rate probes.

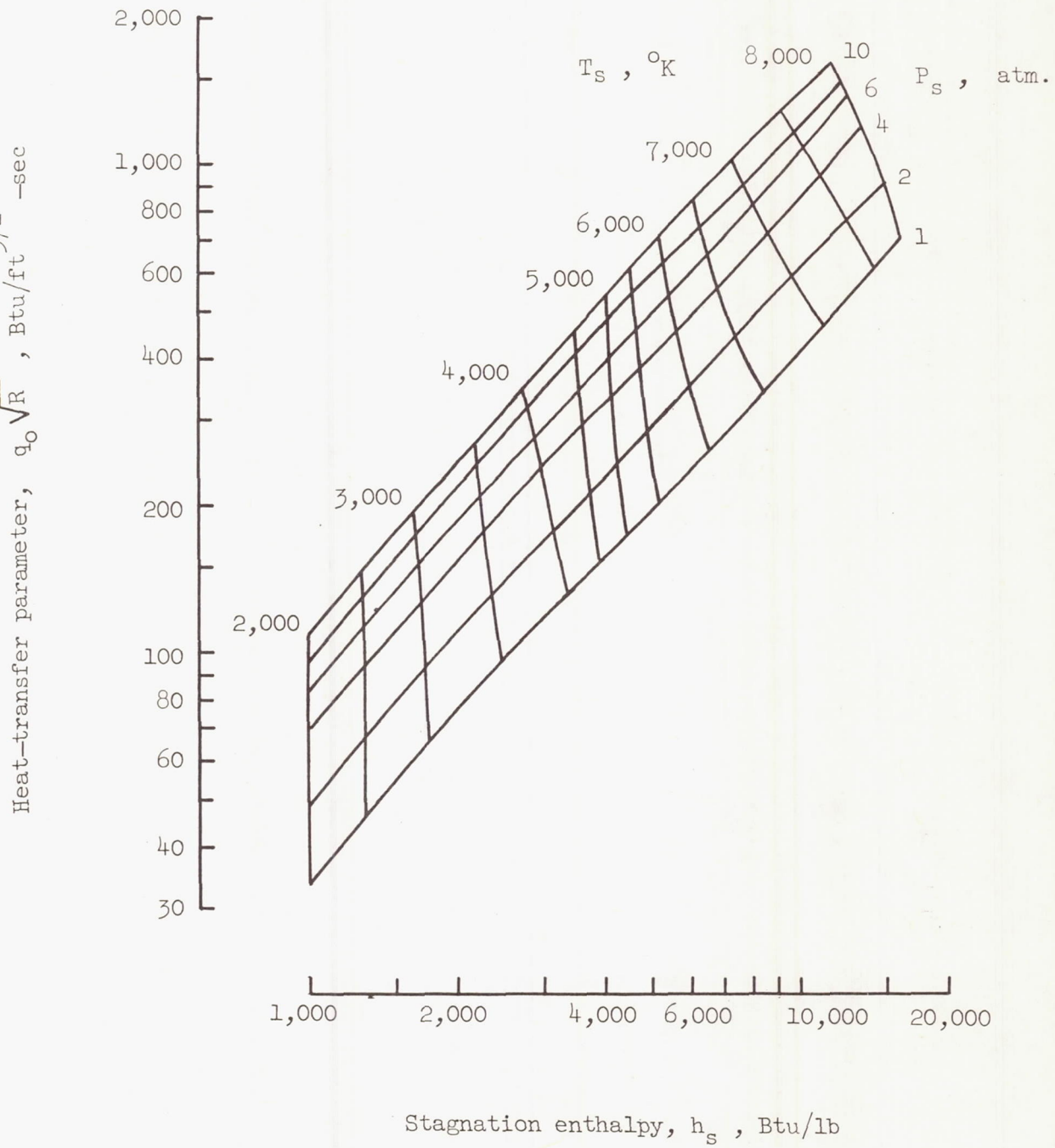

Figure 7.- Heat-transfer parameter as a function of stagnation enthalpy and pressure.

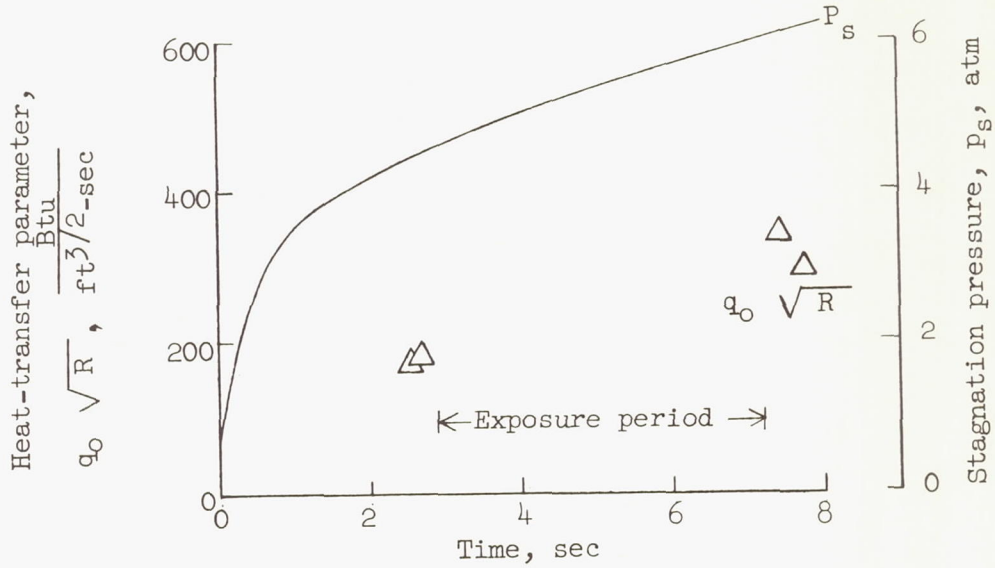

(a) Experimental values.

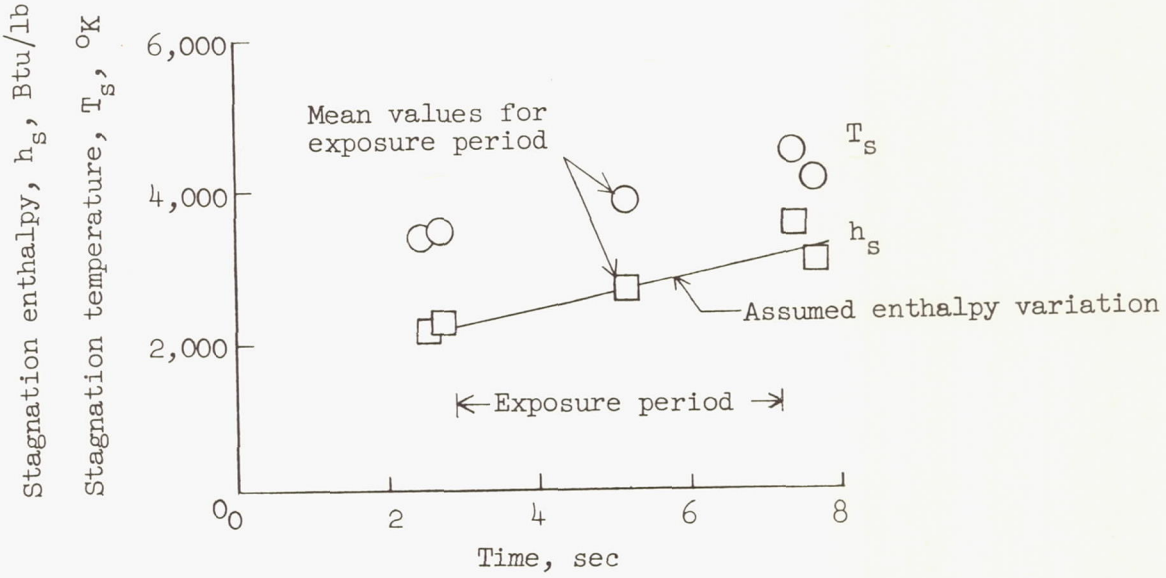

(b) Derived values.

Figure 8.- History of arc-jet stream characteristics for a typical test.

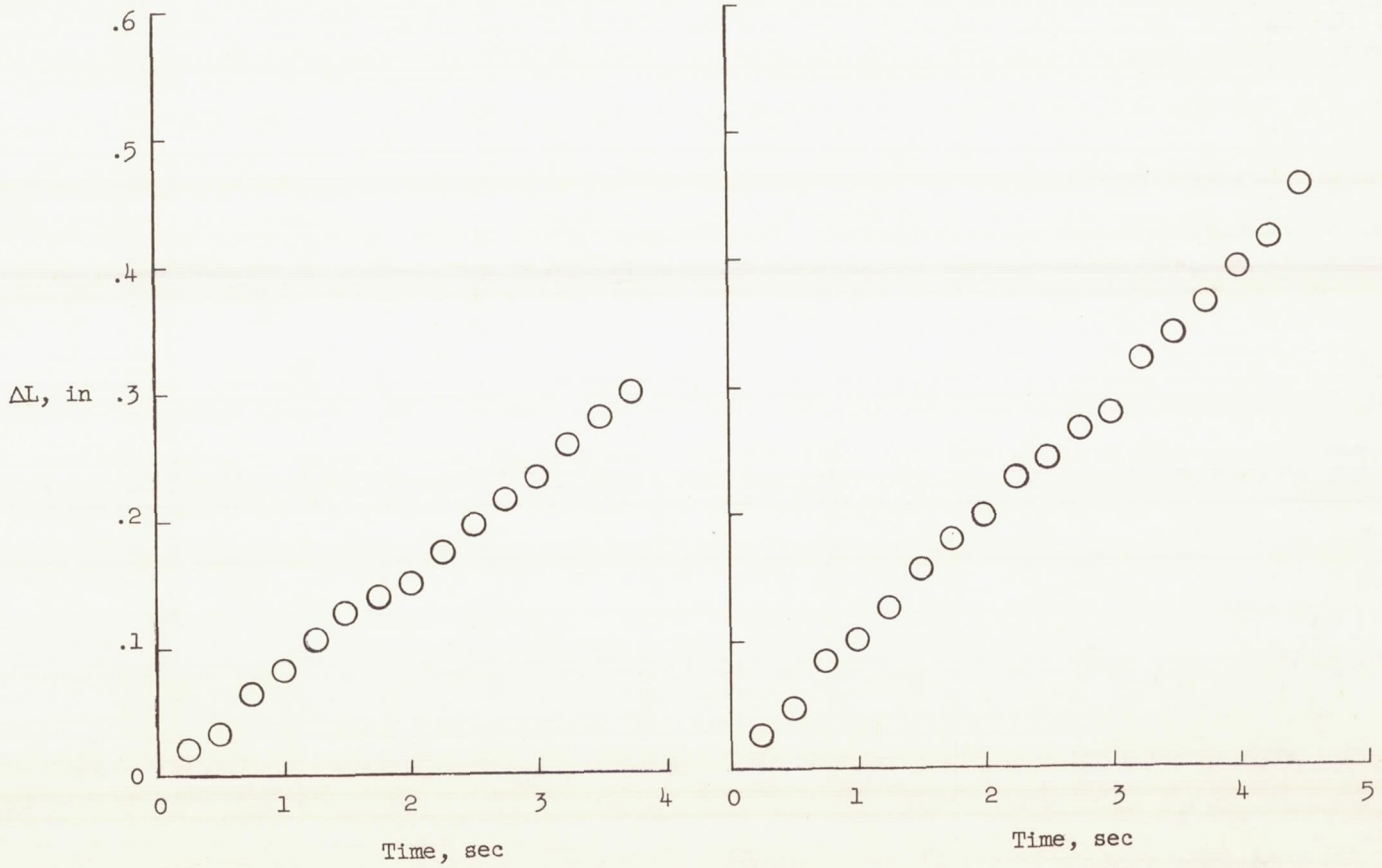

(a) Teflon. $\dot{m}$ = 0.918 lb/ft^2-sec; q'_o = 2,350 Btu/ft^2-sec; h_s = 4,350 Btu/lb.

(b) Ammonium chloride. $\dot{m}$ = 0.775 lb/ft^2-sec; q'_o = 2,870 Btu/ft^2-sec; h_s = 4,900 Btu/lb.

Figure 9.- Length change plotted against time for typical materials tests.

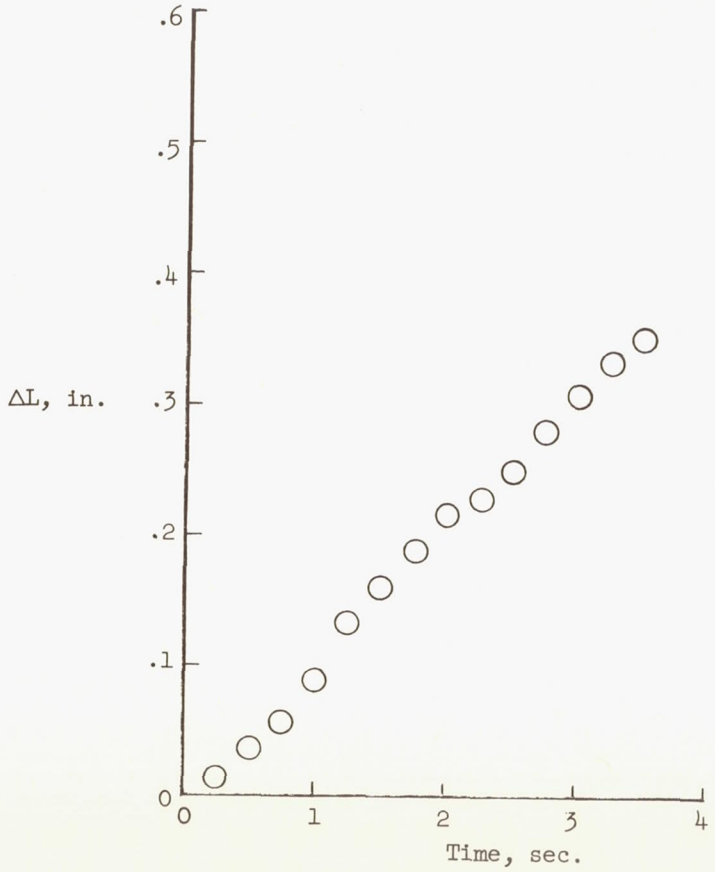

(c) Nylon. $\dot{m}$ = 0.625 lb/ft^2-sec;
q'_o = 1,860 Btu/ft^2-sec;
h_s = 5,200 Btu/lb.

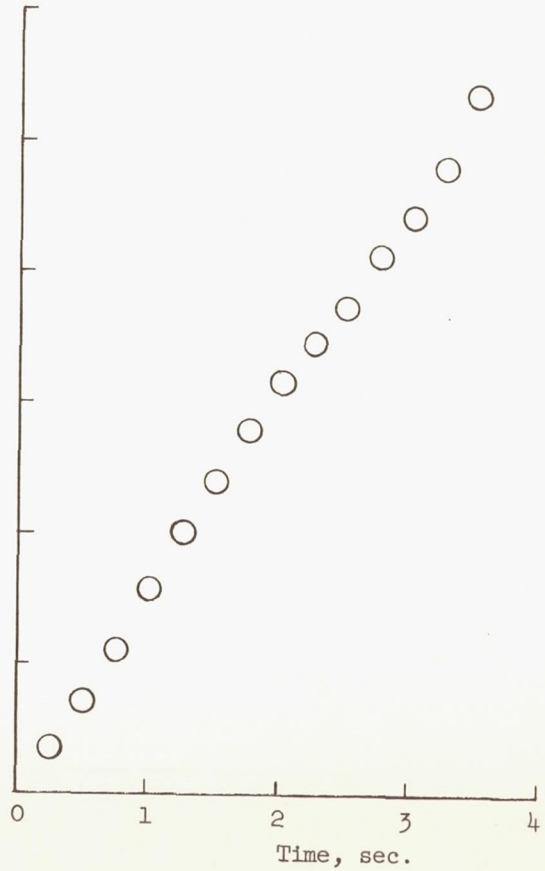

(d) Avcoat 19. $\dot{m}$ = 0.869 lb/ft^2-sec;
q'_o = 2,370 Btu/ft^2-sec;
h_s = 4,200 Btu/lb.

Figure 9.- Continued.

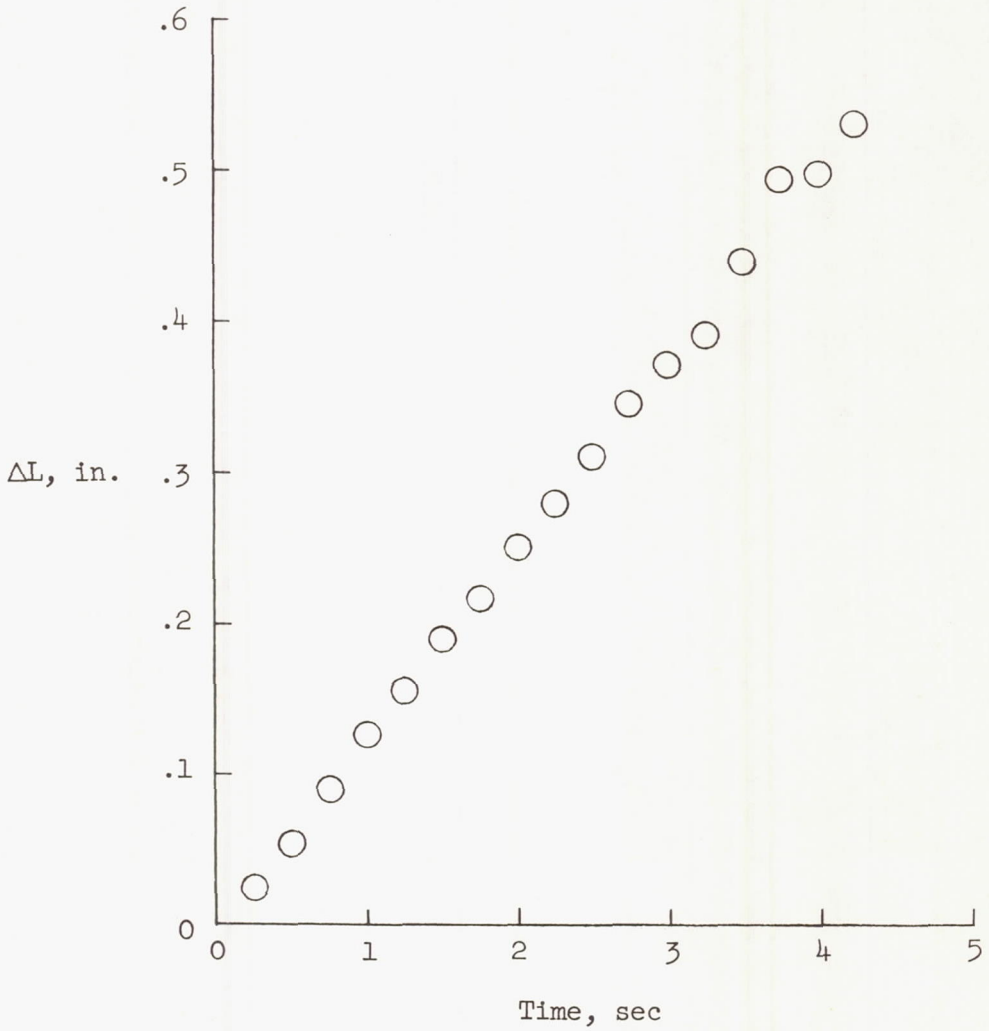

(e) GE-124. $\dot{m}$ = 0.820 lb/ft^2-sec; q'_o = 2,650 Btu/ft^2-sec; h_s = 4,900 Btu/lb.

Figure 9.- Concluded.

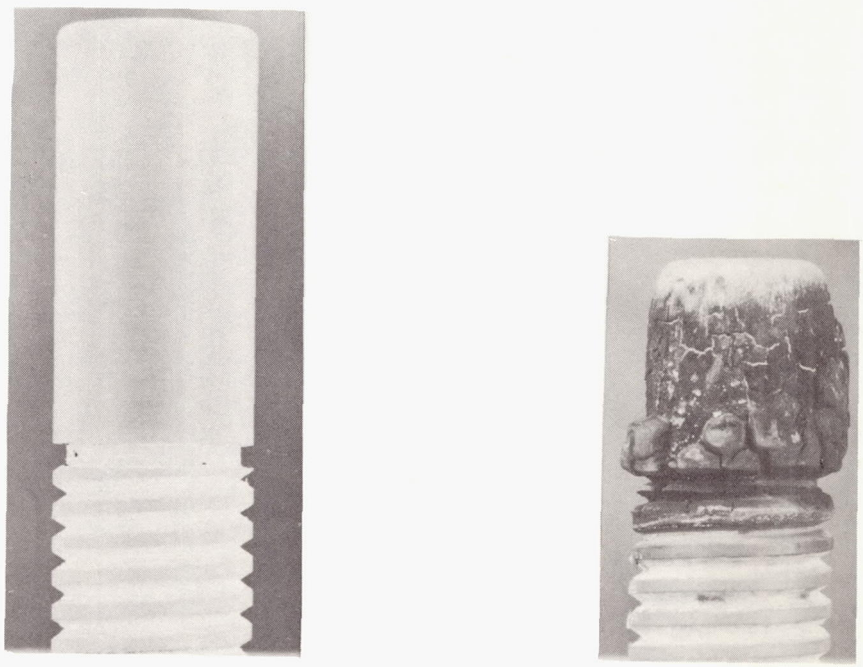

(a) Before exposure.

(b) After exposure.

Figure 10.- Effect of ablation and char removal. GE-124. L-59-8647

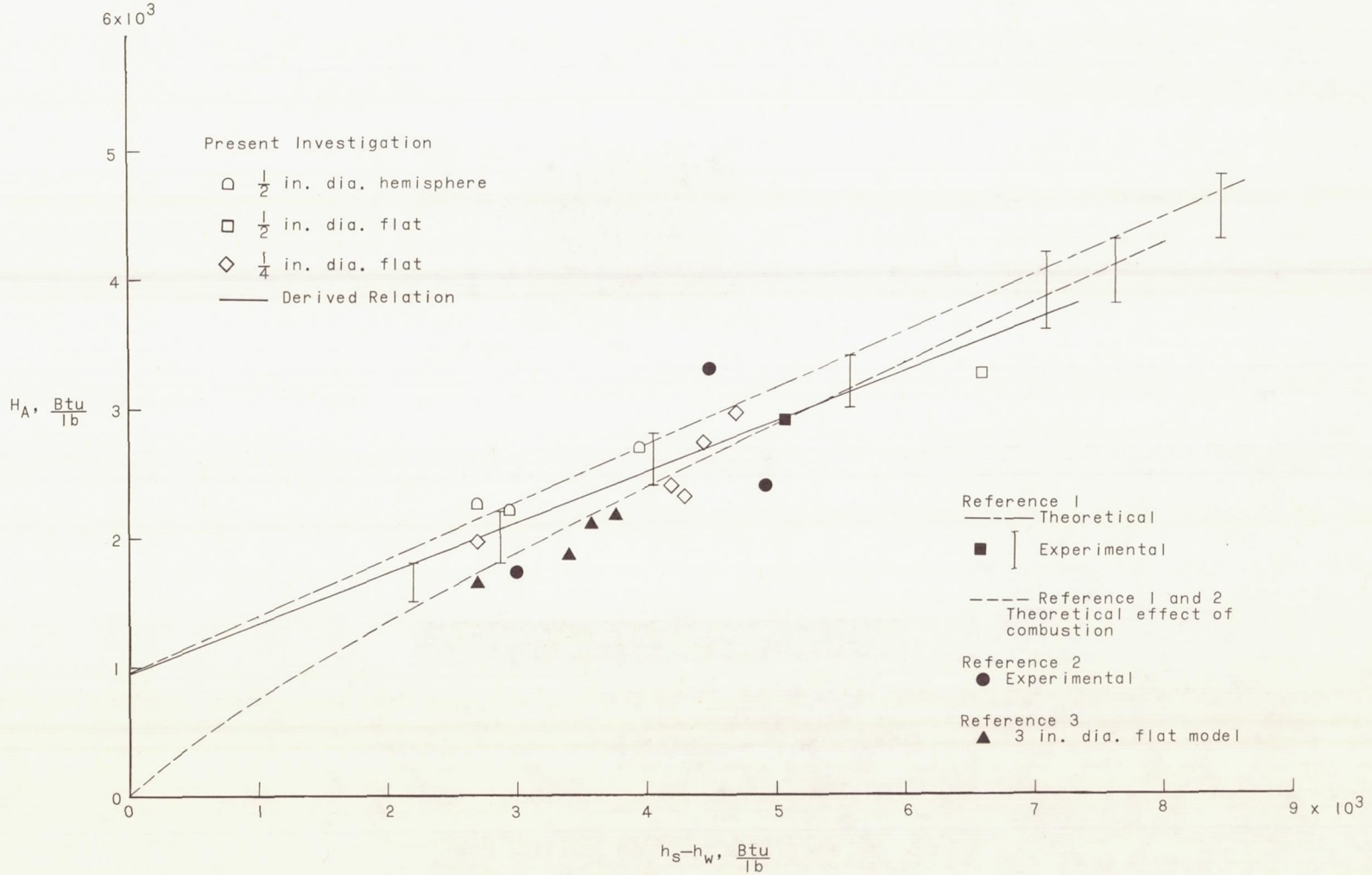

Figure 11.- Heat of ablation plotted against stagnation enthalpy potential. Teflon.

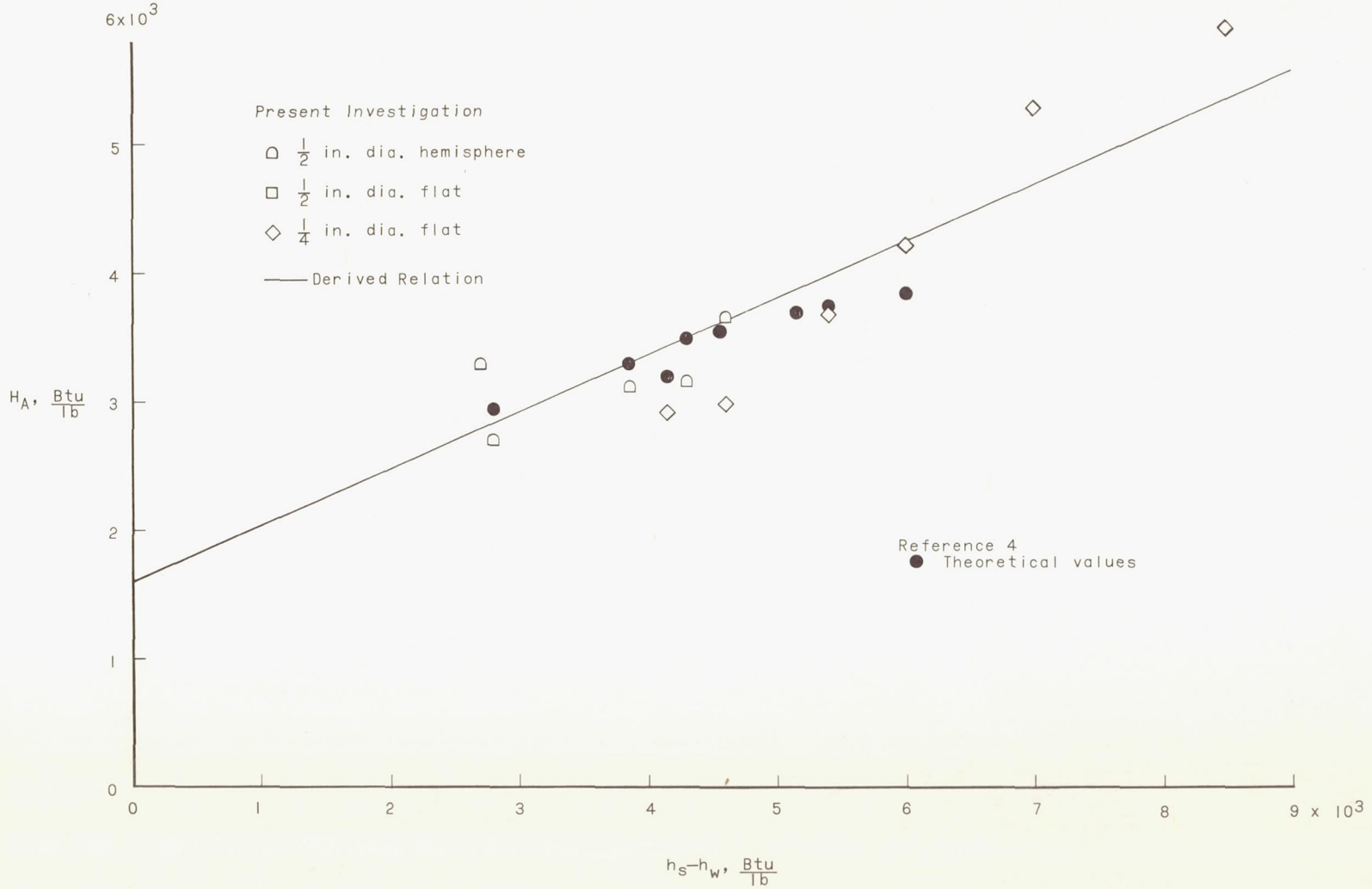

Figure 12.- Heat of ablation plotted against stagnation enthalpy potential. Ammonium chloride.

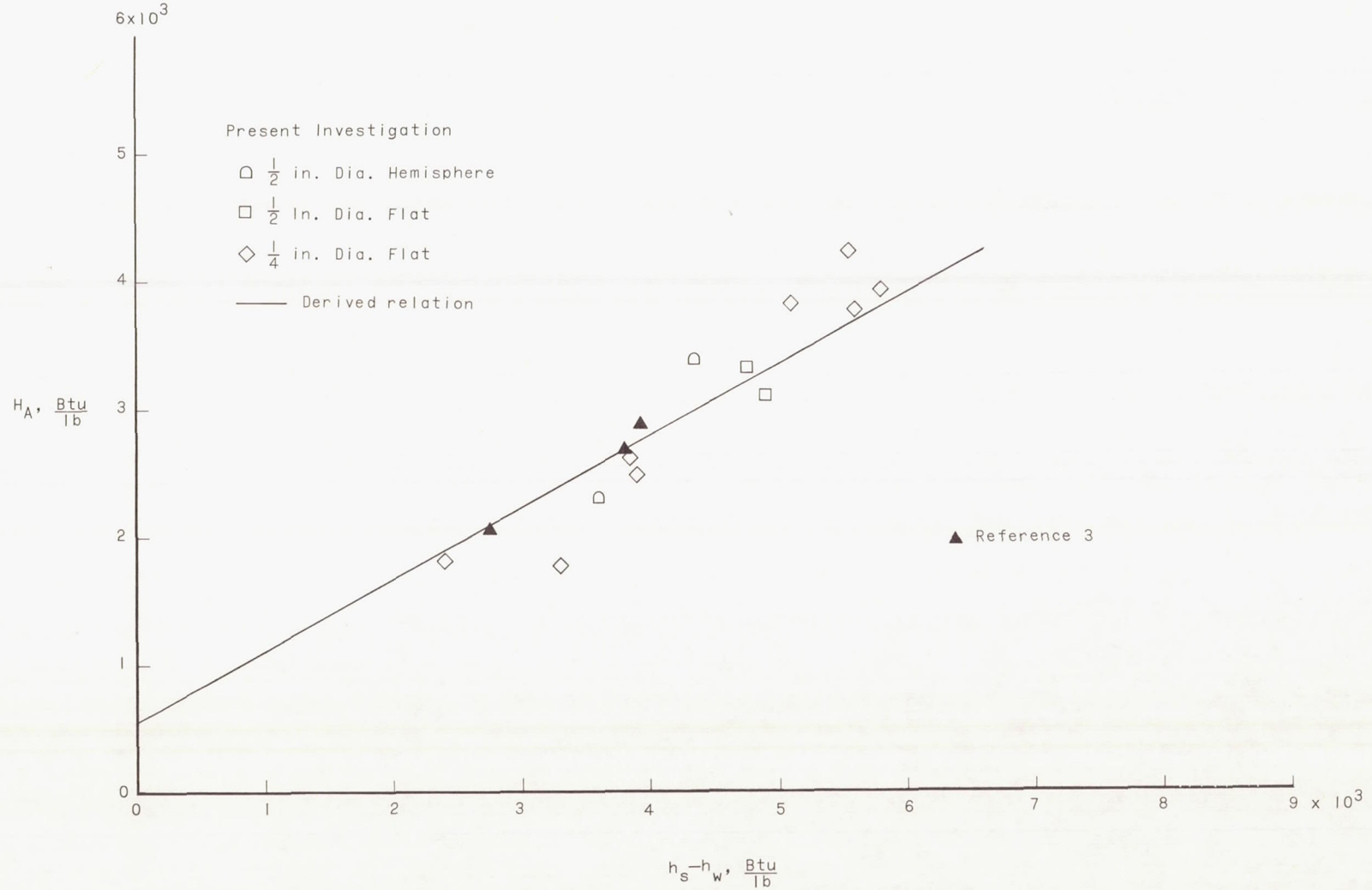

Figure 13.- Heat of ablation plotted against stagnation enthalpy potential. Nylon.

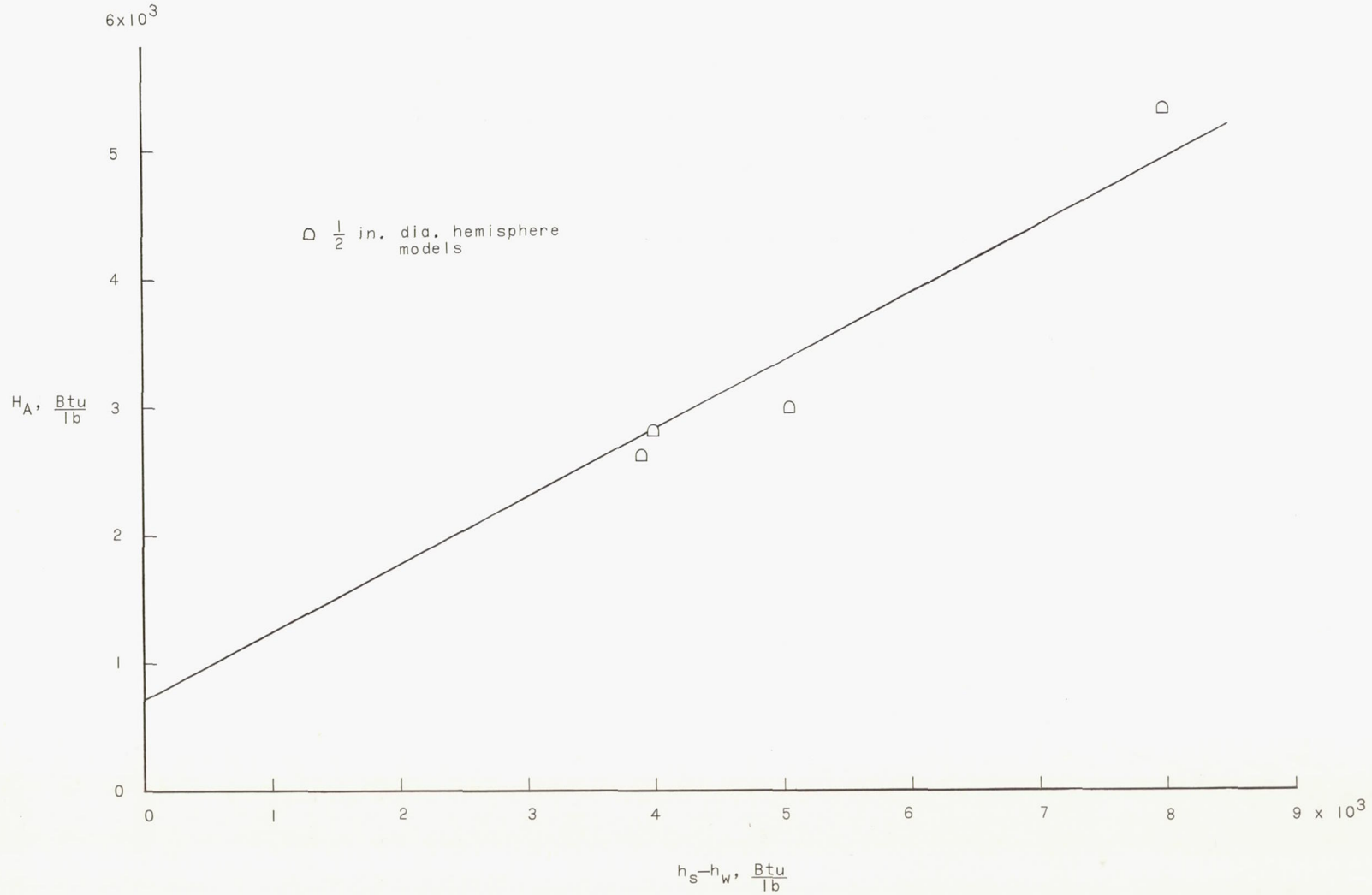

Figure 14.- Heat of ablation plotted against stagnation enthalpy potential. Avcoat 19.

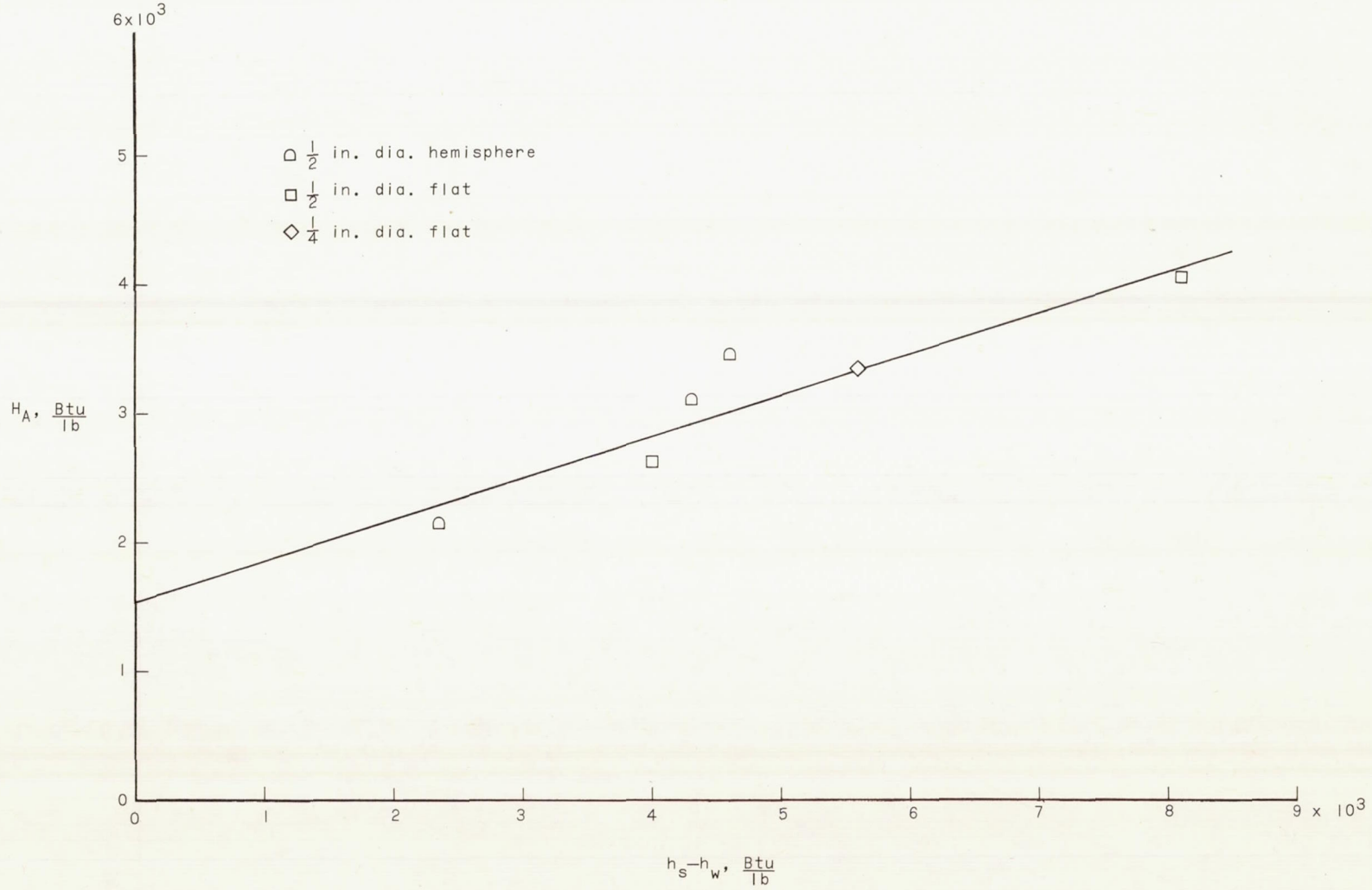

Figure 15.- Heat of ablation plotted against stagnation enthalpy potential. General Electric 124.